Heterogeneity and nearest-neighbor coupling can explain small-worldness and wave properties in pancreatic islets

Giacomo Cappon and Morten Gram Pedersen[a)]
Department of Information Engineering, University of Padua, Via Gradenigo 6/B, 35131 Padua, Italy

(Received 17 February 2016; accepted 29 April 2016; published online 11 May 2016)

Many multicellular systems consist of coupled cells that work as a syncytium. The pancreatic islet of Langerhans is a well-studied example of such a microorgan. The islets are responsible for secretion of glucose-regulating hormones, mainly glucagon and insulin, which are released in distinct pulses. In order to observe pulsatile insulin secretion from the β-cells within the islets, the cellular responses must be synchronized. It is now well established that gap junctions provide the electrical nearest-neighbor coupling that allows excitation waves to spread across islets to synchronize the β-cell population. Surprisingly, functional coupling analysis of calcium responses in β-cells shows small-world properties, i.e., a high degree of local coupling with a few long-range "short-cut" connections that reduce the average path-length greatly. Here, we investigate how such long-range functional coupling can appear as a result of heterogeneity, nearest-neighbor coupling, and wave propagation. Heterogeneity is also able to explain a set of experimentally observed synchronization and wave properties without introducing all-or-none cell coupling and percolation theory. Our theoretical results highlight how local biological coupling can give rise to functional small-world properties via heterogeneity and wave propagation. *Published by AIP Publishing.*
[http://dx.doi.org/10.1063/1.4949020]

The hormone insulin is released in distinct pulses from the β-cells of the pancreatic islets in response to elevated blood glucose levels, and disturbed pulsatile insulin secretion is a hallmark of the metabolic disease diabetes. Electrical coupling between β-cells leads to excitation waves, which have been proposed to provide the synchronizing signal that propagates the glucose-evoked response across the islet. Surprisingly, recent studies showed that the β-cells within an islet constitute a functional small-world network, i.e., a network that shows a high degree of local coupling with a few long-range short-cuts. There are no obvious anatomical candidates for these short-cuts, and further, small-world networks typically do not promote wave propagation. Using computer simulations of a heterogeneously nearest-neighbor coupled lattice network of β-cells, we propose that the functional long-range coupling is due to wave propagation. Further, we show that heterogeneity and gap junction coupling can explain wave and synchronization properties found experimentally without resorting to percolation theory, thus providing a more natural framework for understanding these previous results.

I. INTRODUCTION

Small-world networks[1] have received substantial interest in the last two decades. Such networks are characterized by a high degree of local coupling with a few long-range "short-cut" connections that reduce the average path-length greatly. Global air transportation,[2] co-starring film actors,[1] and the World Wide Web[3] are examples of social and man-made small-world networks. Several biological networks have also been shown to exhibit small-world properties, such as the human brain as revealed by different imaging techniques,[4] the neural network of the nematode worm *Caenorhabditis elegans*,[1] and the metabolic network of *Escherichia coli*.[5] Recently, Ca^{2+} imaging demonstrated that neural progenitors[6] and insulin-secreting pancreatic β-cells[7,8] are functionally coupled in small-world networks.

Functional coupling is derived through pair-wise statistical analysis of the signals from nodes within the network and represents, for example, whether two cells show similar functional behavior. When the correlation of the two signals is above a certain threshold, the nodes are defined to be functionally coupled.[7,9] Mechanistic or physical coupling can be expected to induce functional coupling, but it is not obvious that direct coupling can be inferred from functional coupling; it may be envisaged that two distant nodes appear functionally coupled due to the propagation of a coupling signal via intermediate, directly coupled nodes. In order for the functional signals to be approximately synchronous, so that the nodes are defined as functionally coupled, the coupling signal should propagate fast enough to avoid significant delays compared to the time-scale of the functional signal, e.g., the period of Ca^{2+} oscillations.

Axonal extensions can readily explain the anatomical foundation for the short-cut connections in neuronal small-world networks.[9] In contrast, β-cells are known to be locally coupled by gap junctions formed by connexin-36 (Cx36) proteins, which are crucial for intra-islet synchrony[10] and Ca^{2+} wave propagation.[11,12] Presumably, these excitation waves provide the intra-islet synchrony that, in addition to inter-islet synchrony by unknown signals, is a prerequisite for pulsatile insulin secretion,[13] which is disturbed in

[a)]Electronic mail: pedersen@dei.unipd.it

diabetes.[14] There are no clear candidates for the long-range coupling suggested by functional small-worldness in pancreatic islets,[7,8] though intra-islet neurons and paracrine communication remain possible mediators of long-range coupling.[7] Further, it has been shown that spatiotemporal wave patterns in excitable media may be disrupted by even a low degree of long-range coupling characteristic of small-world connectivity.[15–17] Since inter-cellular Ca^{2+} waves are robustly observed in pancreatic islets,[11,18,19] these results speak against direct long-range coupling between β-cells. Thus, we speculated that functional coupling between distant β-cells is the result of excitation waves spreading via local gap junction coupling,[18] rather than that of physical long-range links.

We investigate this hypothesis with a mathematical model of heterogeneously gap-junction-coupled β-cells in a regular lattice network. We show that nearest-neighbor coupling can result in small-world characteristics of the network when investigated with "functional coupling." Moreover, our simulations show that synchronization and wave properties of islet Ca^{2+} dynamics[11] can be explained by heterogeneity and ohmic gap junction coupling. Our results prove that functional small-worldness is not necessarily a result of anatomical or mechanistic small-worldness.

II. RESULTS

We performed simulations of electrically coupled beta-cells, each modeled by a general and commonly used mathematical description of bursting electrical activity and Ca^{2+} oscillations.[20] The cells were organized in a hexagonal lattice[21] where a center cell has 12 neighbors. Cell parameters and coupling strengths were distributed randomly, in particular, the findings that only ~67% of adjacent cells (possible cell pairs) are gap-junction coupled[22] were taken into consideration. As a result, a center cell was on average coupled to ~8 cells, in good agreement with estimations from whole-islet patch clamp recordings.[23]

Our aim was to investigate if such an arrangement can explain, simultaneously, wave propagation commonly seen in pancreatic islets[11,18] and small-world properties of the cell network defined by functional coupling.[7,8] Further, we were interested in studying the origin of synchronization and wave properties when gap junction coupling strength was modified.[11]

For this latter purpose, pharmacological or genetic reduction of the gap junction conductances was assumed to be heterogeneous, reducing the coupling strength between individual pairs of cells unevenly. This assumption reflects that the degree of pharmacological inhibition of gap junction channels most likely various from one cell pair to another. Similarly, $Cx36^{+/-}$ cells were assumed to have some cell-to-cell variation around the 50% reduction in the number of gap junction channels expected from the heterozygous genotype, which could be due to the differences in post-processing, protein transportation, and formation of functional gap junctions. Such heterogeneity was modeled by multiplying individual conductances with randomly distributed constants drawn from a distribution with mean μ between 0 and 1, and standard deviation 0.2 (see Sec. IV). The drawn constants were truncated to guarantee that they fell within the interval [0, 1].

We analyzed our simulations following the approach of Benninger *et al.*[11] in order to facilitate comparison with their experimental results (see Sec. IV for details). We found that Ca^{2+} waves propagated across the islet (Fig. 1), and that the wave speed was reduced when gap junction conductance was diminished (Fig. 2(a)). Below a certain average gap junction strength ($\mu \approx 0.4$), wave propagation no longer

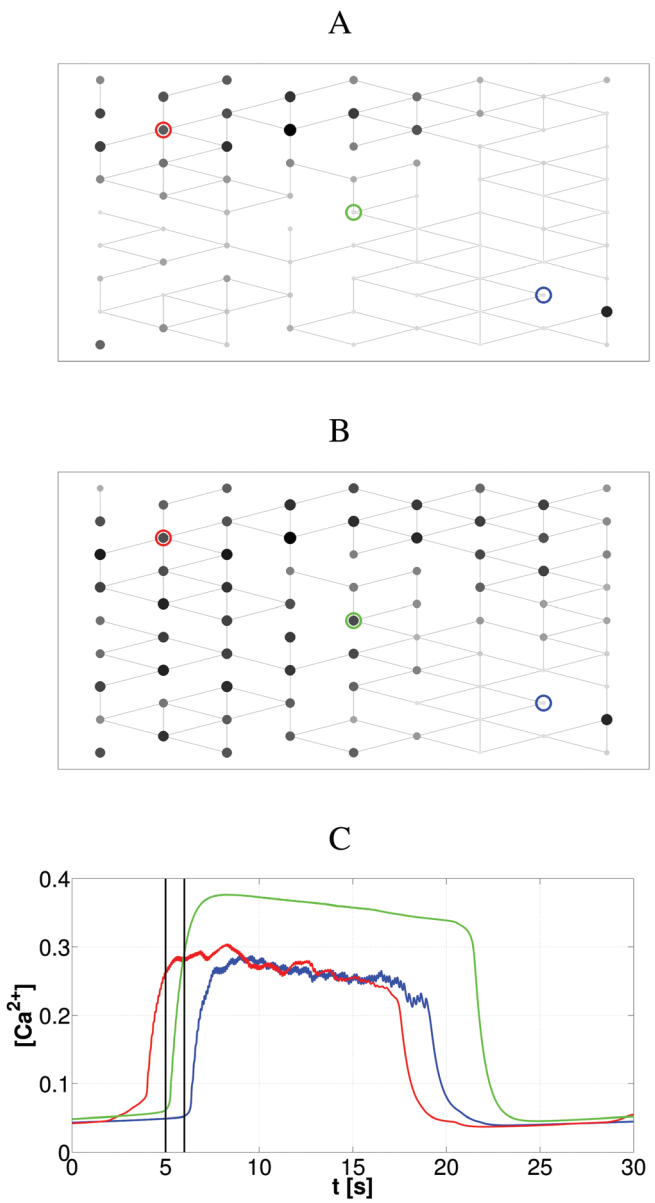

FIG. 1. Wave propagation. (a) A snapshot of a center plane of a three-dimensional hexagonal lattice of simulated β-cells (nodes) with $\mu = 0.8$ at time $t = 5$ s. The edges indicate whether two neighbor cells are directly coupled ($g_{ij} > 0$ pS). Note that coupling may occur via adjacent layers. The size of the nodes and the intensity of the shade of grey indicate the simulated Ca^{2+} level at the given time point. The colored circles indicate cells for which Ca^{2+} traces are shown in panel (c). (b) As in panel (a), but at time $t = 6$ s. Note that the Ca^{2+} wave has propagated from the upper left towards the lower right. (c) Simulated Ca^{2+} traces of the three cells indicated in panels (a) and (b) by the correspondingly colored circles. The vertical lines indicate the times of the snapshots shown in panels (a) and (b).

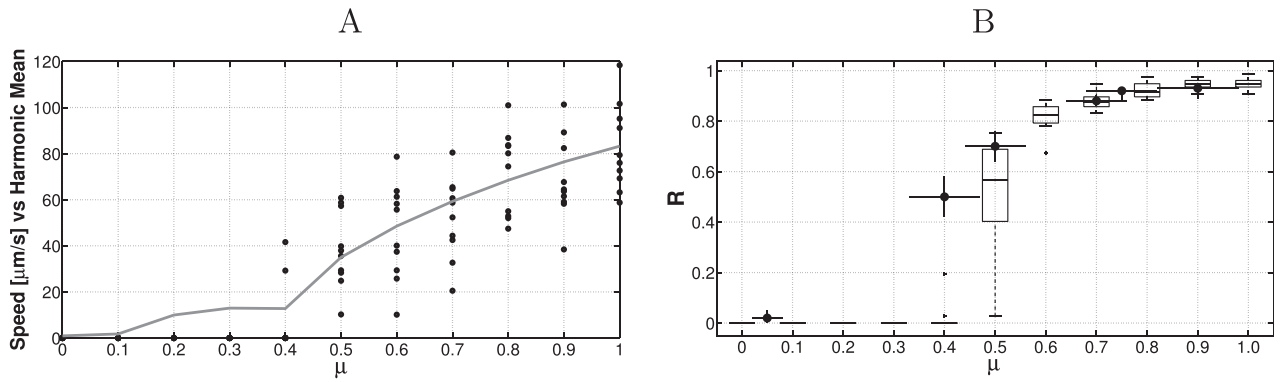

FIG. 2. (a) Calculated wave speeds for 10 simulated islets for each value of μ (dots), and scaled square-roots of the weighted harmonic means of the positive gap junction conductances, averaged over the 10 β-cell networks (gray curve). (b) Synchronization measured as the fraction of cells with peak cross-correlation coefficient >0.85 in 10 simulations for each value of μ (box plots), and corresponding experimental data (points with error bars) taken from Benninger *et al.*[11]

occurred, in agreement with previous simulations.[11] Heterogeneity is crucial for understanding this observation,[24] since in the case of homogeneous cell properties and gap junction coupling the wave speed is proportional to the square root of the coupling strength[11,18] and allows wave propagation also for very small gap junction conductances (Fig. S1 in the supplementary material[25]). In contrast, with heterogeneity, the wave speed is approximately proportional to the square root of the harmonic mean of the coupling strengths,[24] which can be very small even when the average coupling strength is well above zero. Indeed, the wave speeds in our simulations were approximately proportional to the square-root of the harmonic mean of the positive gap junction conductances weighted by the fraction of positive conductances (Fig. 2(a), see also Sec. IV).

The model simulations also reproduced the islet synchrony properties as gap junction conductance was varied (Fig. 2(b)).[11] In this approach, the cross-correlation between each of the simulated single-cell Ca^{2+} traces and the average islet Ca^{2+} signal was calculated, and the degree of synchrony was defined as the fraction of cells having peak cross-correlation coefficient >0.85 (see Sec. IV and Ref. 11). Confronting panels (a) and (b) in Fig. 2 suggests that the propagating waves are responsible for synchronizing the β-cell population in our simulations. Thus, heterogeneous gap junction coupling can explain wave and synchrony properties at changing gap junction coupling strengths.

We proceeded by analyzing the correlation between Ca^{2+} oscillations in the cells, following the recipe of Stožer *et al.*[7] Pair-wise cross-correlation coefficients were calculated for the simulated cellular Ca^{2+} traces after discarding initial transients (see Sec. IV for details). If the Ca^{2+} oscillations of two cells showed correlation above a threshold level, then these cells were defined to be functionally coupled. Thus, from this analysis, we obtained a graph with nodes representing cells, and all-or-none edges indicating whether two nodes (cells) were functionally coupled (Fig. 3(a)). The graph was then analyzed with techniques from network theory. In particular, we calculated the average clustering coefficient C, which measures the degree of local coupling in the network, and the efficiency E, an indicator of how well information is transferred across the network.[9,26] We then

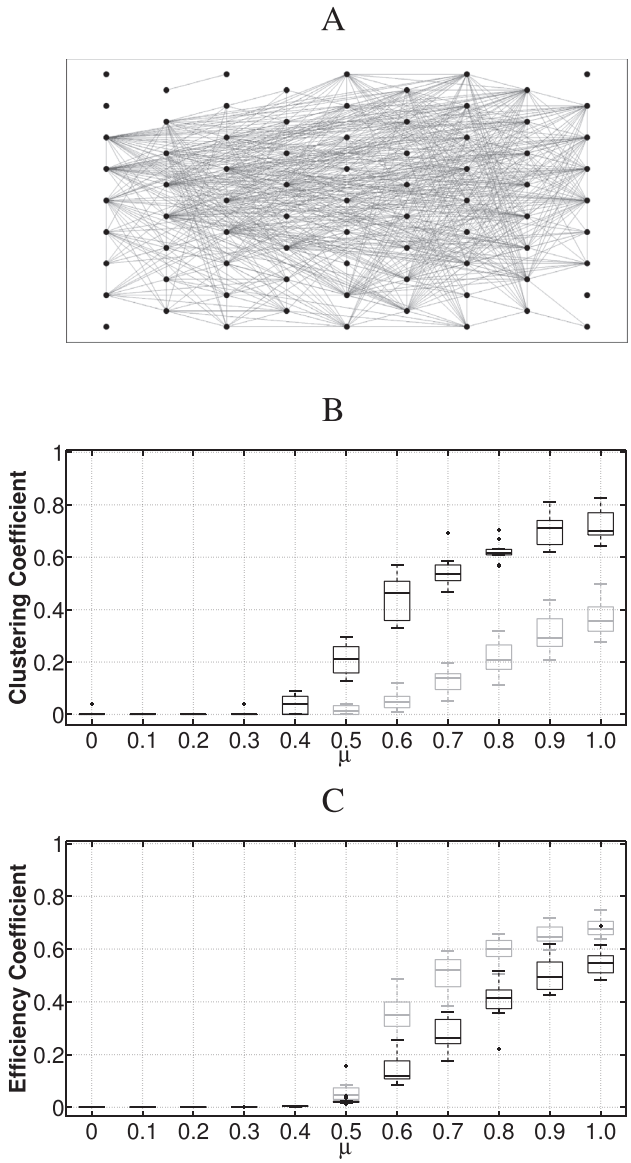

FIG. 3. Functional coupling and small-worldness. (a) An example of a functional network of β-cells. The same plane of simulated β-cells shown in Fig. 1 was analyzed as explained in Sec. IV; functional coupling is indicated by edges between nodes (cells). (b) Clustering coefficients for varying coupling strength. The box plots indicate the results of 10 simulated β-cell networks (black) and 10 corresponding random networks (gray). (c) As in panel (b), but showing the efficiencies.

TABLE I. Functional network parameters. The values are medians of values obtained from 10 simulated β-cell networks and 10 corresponding random graphs.

μ	C	C_r	C/C_r	E	E_r	E_r/E	S
0.6	0.46	0.05	10.35	0.05	0.12	2.67	3.88
0.8	0.62	0.21	3.10	0.41	0.60	1.44	2.15
1.0	0.70	0.36	2.01	0.55	0.68	1.24	1.61
Stožer *et al.*[7]	0.67	0.12	5.59	0.29	0.41	1.41	3.96

confronted these indices with indices obtained from a graph with the same number of nodes and edges (degree), but where the nodes were linked randomly (Erdös-Renyi graph). Small-world networks are defined by having efficiency similar to random networks ($E \approx E_r$) due to long-range connections, whereas the average clustering coefficient is much higher, reflecting that small-world networks locally (in topological sense) are similar to lattice networks.[1] These conditions are often condensed into the index $S = (C/C_r)/(E_r/E)$, and small-worldness is defined[7] as $S > 1$.

Table I confronts the results of our simulations with the results from Stožer *et al.*[7] We find that our simulations exhibit indices similar to the experimentally obtained ones with the best correspondence for $\mu = 0.8$. In particular, our nearest-neighbor coupled network shows small-worldness with respect to functional coupling, although the S value tends to be slightly below the experimental value. For $\mu = 0.8$, this is entirely due to a too high average clustering coefficient for the random networks (C_r). All together, our results highlight that functional small-worldness does not necessarily imply direct long-range coupling, but that such long-range *functional* coupling can result, for example, from excitation wave propagation between nearest neighbors.

To investigate this idea further, we analyzed the graphs defined by functional coupling as the gap junction coupling strength was varied, which, as discussed above, change the wave properties.[11] We found that the clustering coefficient C was greater than the corresponding random network, $C > C_r$, for $\mu > 0.4$ (Fig. 3(b)). In contrast, the networks of β-cells had similar, or slightly lower, efficiencies than the corresponding random networks for $\mu > 0.4$, $E \sim E_r$ (Fig. 3(c)). Thus, $S > 1$ for $\mu > 0.4$ indicating small-worldness in the simulated β-cell network. Note that this range of gap junction coupling strength corresponds to the values where wave propagation and synchrony are obtained (Fig. 2), suggesting that the concepts of wave propagation, functional coupling, and small-worldness are intimately related.

III. DISCUSSION

In this work, we have investigated the influence of heterogeneity and gap junction coupling between simulated β-cells with attention to wave propagation, synchronization, and small-world properties. We were able to reproduce apparently unrelated experimental results regarding, respectively, synchrony and wave propagation[11] or small-world network properties[7,8] in a unifying framework consisting of a lattice of coupled β-cells.

We suggest that wave propagation is the key to explain the findings. First, synchronization is related to whether wave propagation is present or not, both in experiments[11] and in our simulations (Fig. 2). Second, we found that distant cell was functionally coupled in spite of the imposed nearest-neighbor coupling (compare edges in Figs. 1(a) and 3(a)). Likely, the observed excitation waves provide the communication between these distant cells, yielding the near-synchrony that results in functional coupling when the simulated Ca^{2+} traces are analyzed. These long-range short-cuts in the functional network (Fig. 3(a)) assure that the efficiency is similar to the corresponding random networks (Fig. 3(c) and Table I). The efficiency is a measure of how efficiently the network transports information. In the case of pancreatic islets, it has been suggested that wave propagation is a means to communicate a glucose stimulus between β-cells.[18] Our results show that the networks of nearest-neighbor coupled β-cells have efficiencies approaching the efficiencies of the corresponding random graphs (Fig. 3(c)), which suggest that the excitation waves transport information, such as the presence of glucose stimuli, between cells almost as efficiently as random networks.

In contrast, the clustering coefficient was higher in our simulations than in the corresponding random networks for the entire range of coupling strengths permitting wave propagation ($\mu > 0.4$, Fig. 3(b)), which together with the efficiency results lead to the small-world property in our simulations (Table I) in agreement with experimental findings.[7] The high clustering coefficient is what is to be expected in a lattice network as simulated here. In biophysical terms, the small-world property means that neighboring cells, because of direct gap-junction coupling, are easily synchronized (high clustering coefficient) but some distant cells are also synchronized because of wave propagation (long-range short-cuts and high efficiency).

We propose that it is heterogeneity and gap junction coupling that determine the wave speed and the degree of synchrony in the network (Fig. 2) when the coupling strength varies. Previous simulations of wave propagation between heterogeneous, gap junction coupled β-cells agree with the results presented here,[11] but were interpreted using percolation theory, which considers and modifies the fraction of all-or-none coupling to model changes in average gap junction conductance. In our opinion, this interpretation is biologically less realistic than our view focusing on heterogeneity, and moreover, does not correspond to the simulations. Indeed, the number of missing connections is constant in our simulation for $\mu \geq 0.4$ (Fig. 4), i.e., the range where wave speed, the fraction of synchronized cells, and the clustering coefficient and efficiency vary (Figs. 2 and 3). Note also that we are far from the percolation threshold for hexagonal three-dimensional lattices ($p_c = 0.12$, i.e., 88% missing connections[27]) in all our simulations (Fig. 4).

To understand how the wave speed changes with coupling strength, heterogeneity is crucial. If both cell parameters and coupling are homogeneous, the wave speed follows the square-root of the gap junction conductance,[11,18] and

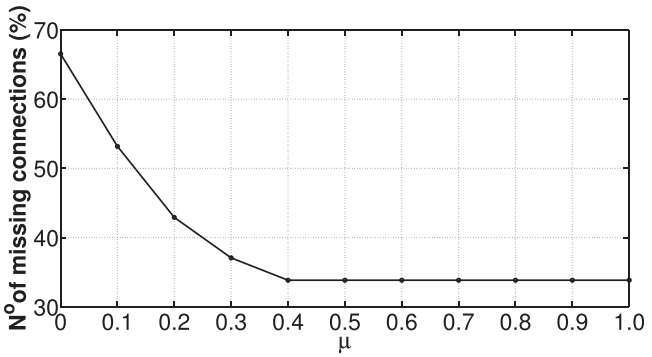

FIG. 4. Heterogeneity, not missing connections, explains the results. The number of missing connections, calculated as the fraction of neighboring cell pairs where the reduced coupling strengths $k_{ij}g_{c_{ij}}$ equal zero, is virtually constant in the range $\mu \in [0.4, 1]$ where the wave speed, synchrony, and network properties vary. Note also that we are below the percolation threshold of ~80% missing connections for all values of μ.

wave propagation is seen even for low coupling strengths (Fig. S1), in contrast to experiments.[11] Cell-to-cell variation in intrinsic cell parameters can give results similar to experimental findings even in the presence of (biologically unrealistic) homogeneous electrical coupling (Fig. S2). Of note, the threshold for wave propagation and synchrony is not due to percolation failure, since the number of missing connections was kept constant at 33%, well below the percolation threshold.[27] Previous studies of coupled heterogeneous β-cells similarly found that the cell population did not synchronize at low coupling strengths, and moreover that this finding did not depend on whether gap junction coupling was assumed heterogeneous or homogeneous.[28] Simulations of heterogeneous cardiac or Fitzhugh-Nagumo cells with homogeneous coupling also showed that a certain coupling strength is needed to permit wave propagation and synchrony.[29] Thus, the presence of a coupling threshold below, which wave propagation is absent, is not strictly dependent on the presence of heterogeneous coupling, if the cell population is heterogeneous.

Finally, assuming homogeneous reduction in the gap junction strength, modeled as $k_{ij} = \mu$ with no variation, yielded results (Fig. S3) similar to the ones presented in the figures above, since the cells and electrical coupling were already heterogeneous. However, in our opinion, non-homogeneous pharmacological inhibition of gap junctions is the more realistic assumption. In the presence of heterogeneous coupling, the wave speed has been predicted to be proportional to the square-root of the harmonic mean of the gap junction conductances,[24] which is influenced not only by the average conductance but also by the degree of heterogeneity (the variation of the gap junction conductance distribution of the islet). Indeed, the square-root of the calculated harmonic mean predicts the simulated wave speeds decently (Fig. 2(a)). The complete absence of wave propagation below a certain coupling strength in spite of positive harmonic mean is likely due to the discrete and heterogeneous structure of the cellular network, since it was also observed with homogeneous coupling (Fig. S2) and in the case of even reduction of the gap junction conductance (Fig. S3), is in agreement with previous results.[11,28,29]

In summary, our simulations highlight that wave propagation can provide the mechanism of long-range synchronization in pancreatic islets with no need for direct links between distant β-cells. Besides synchronizing the β-cell population, the excitation waves lead to short-cuts in the functional coupling graph, which, in combination with the underlying lattice structure and local gap junction coupling, result in functional small-worldness. Heterogeneity can further explain why a certain degree of coupling is needed for wave propagation and synchrony, and how the wave speeds vary with average coupling strength, without assuming that such behavior results from a change in the number of missing connections between neighbors as in percolation theory.

IV. METHODS

A. Model

We model a heterogeneous population of β-cells arranged in a hexagonal lattice.[21] Each cell is represented by a general and widely used β-cell model,[20] consisting of descriptions of the membrane potential V, the intracellular Ca^{2+} concentration Ca, four ionic membrane currents, and passive nearest-neighbor gap junction currents. Cellular heterogeneity was imposed by random generation of the parameters according to a normal distribution with 10%–20% standard deviation, except for the gap junction conductances ($g_{c_{ij}}$), which have 50% standard deviation. In case the algorithm drew a value for $g_{c_{ij}} < 0$ pS, the conductance was set to 0 pS to avoid negative conductances. Further, 33% of the $g_{c_{ij}}$ values were randomly selected and set equal to zero.[22] Such cases ($g_{c_{ij}} = 0$ pS) correspond to missing coupling between adjacent cells in experiments.[22] We refer to the supplementary material[25] for details on network construction, equations, and parameters. Control simulations confirmed that similar results were obtained with networks of different size (Fig. S4) or when using a cubic lattice (Fig. S5).

To model pharmacological or genetic modification of the gap junction conductances,[11] we multiplied each $g_{c_{ij}}$ by a coefficient k_{ij}, normal distributed with mean $\mu \in [0, 1]$ and standard deviation 0.2. This assumption reflects pharmacological inhibition of an uneven number of connexons between cell pairs, or heterogeneous connexin 36 expression in the case of $Cx36^{+/-}$ animals.[11] The algorithm assures that each k_{ij} is assigned a value between 0 and 1 by setting $k_{ij} = 1$ if a value > 1 is drawn, and $k_{ij} = 0$ if a negative value is drawn. Missing coupling between cells i and j can thus occur either as a result of missing gap junction channels ($g_{ij} = 0$ pS) or because of complete inhibition ($k_{ij} = 0$). The frequency of such cases ($k_{ij}g_{ij} = 0$ pS) is shown in Fig. 4.

Simulations were performed in MATLAB using the ode45 solver. Computer code is available from http://www.dei.unipd.it/~pedersen.

B. Analysis

All analyses were performed on a sheet of 77 cells (see Fig. 1(a)) to mimic the typical experimental setting.[7,11] The simulated islets were composed of 1643 cells.

1. Wave propagation

We measured the wave propagation velocity as Benninger *et al.*:[11] first, for each simulated cell, we computed the cross-correlation between the time course of its Ca^{2+} level and the average Ca^{2+} trace for the simulated islet. We defined the time delay Δt_i of a given cell i as the time index of its cross correlation-peak, so that a low (negative) time index represents an earlier increase in $[Ca^{2+}]$, while a higher (positive) time index indicates a later $[Ca^{2+}]$ rise. We also used the cross-correlation peak value to determine whether a given cell was synchronized or not (see Sec. IV B 2 below).

Following the method in Ref. 11, we defined the start and end cells of the Ca^{2+} waves as the synchronized cells with the minimum and the maximum delay, respectively. The start and end cells thus varied between simulated islets, but were identical for the waves occurring in each simulated islets. The wave speed is calculated as

$$v_{Ca} = \frac{\Delta s_{12}}{\Delta t_{12}}, \tag{1}$$

where Δt_{12} and Δs_{12} represent, respectively, the difference in time delays and the distance between the start and end cells.

To evaluate the proportional relation between simulated wave speeds and coupling strengths, we computed the square-root of the harmonic mean of its positive gap junction values ($g_{c,k}$), taking into account the fraction of gap junction values equal to zero

$$HM = \frac{N_Z}{N_W}\left(\frac{1}{N_Z}\sum_{k=1}^{N_Z}\frac{1}{g_{c,k}}\right)^{-1}, \tag{2}$$

where N_W is the total number of gap junctions and N_Z is the number of gap junctions with positive conductance. The square-roots of calculated HM values, scaled appropriately, are shown in Fig. 2(a).

2. Synchrony

In order to understand if the i-th cell is synchronized to the whole islet cluster, we compute the cross-correlation between its $[Ca^{2+}]$ time course and the islet average $[Ca^{2+}]$ time course. If the maximum value of the computed cross-correlation coefficient is >0.85, then the i-th cell is considered synchronized with the islet.[11] To evaluate the cluster synchronization level, we compute the fraction of synchronized cells $R = n_s/N$, where n_s is the number of cells considered to be synchronized and N is the total number of cells.

3. Functional coupling and network analysis

Given an islet we obtained its functional coupling graph by two steps.[7] We computed the cross-correlation coefficients P_{ij} between simulated Ca^{2+} traces in pairs of cells. Cells i and j were considered functionally coupled if and only if $P_{ij} > 0.95$, corresponding to an edge between nodes i and j in the functional graph. The clustering coefficient of the i-th node (cell), C_i, is defined as the number of existing connections between all neighbors of a node, divided by the number of all possible connections between them, and the average clustering coefficient, C, is the average of C_i over all nodes.[1,7,9] The global efficiency E is a measure of how efficient the network transports information and is inversely related to the average shortest path length.[7,9,26] We used the The Brain Connectivity MATLAB Toolbox (http://www.brain-connectivity-toolbox.net) to calculate C and E for functional graphs obtained from the simulated β-cell networks. In the same way, we obtained the corresponding indices C_r and E_r for random networks with the same degree as the functional graphs. Small-world networks are locally lattice-like yielding a high average clustering coefficient, $C \gg C_r$, but have long-range short-cuts giving a high efficiency, $E \sim E_r$. The small-worldness parameter S is defined as $S = \frac{C_{avg}}{C_{rand}} / \frac{E_{rand}}{E_{glob}}$. For a small-world network, $S > 1$.

ACKNOWLEDGMENTS

M.G.P. was supported by the University of Padua (Strategic Project DYCENDI).

G.C. performed the research and prepared the figures. M.G.P. conceived and designed the research, analyzed data, and wrote the paper.

[1]D. J. Watts and S. H. Strogatz, "Collective dynamics of 'small-world' networks," Nature **393**, 440–442 (1998).
[2]R. Guimerà, S. Mossa, A. Turtschi, and L. A. N. Amaral, "The worldwide air transportation network: Anomalous centrality, community structure, and cities' global roles," Proc. Natl. Acad. Sci. U. S. A. **102**, 7794–7799 (2005).
[3]L. A. Adamic, "The small world web," in *Research and Advanced Technology for Digital Libraries* (Springer, 1999), pp. 443–452.
[4]C. J. Stam, "Modern network science of neurological disorders," Nat. Rev. Neurosci. **15**, 683–695 (2014).
[5]A. Wagner and D. A. Fell, "The small world inside large metabolic networks," Proc. Biol. Sci. **268**, 1803–1810 (2001).
[6]S. Malmersjö, P. Rebellato, E. Smedler, H. Planert, S. Kanatani, I. Liste, E. Nanou, H. Sunner, S. Abdelhady, S. Zhang, M. Andäng, A. El Manira, G. Silberberg, E. Arenas, and P. Uhlén, "Neural progenitors organize in small-world networks to promote cell proliferation," Proc. Natl. Acad. Sci. U. S. A. **110**, E1524–E1532 (2013).
[7]A. Stožer, M. Gosak, J. Dolenšek, M. Perc, M. Marhl, M. S. Rupnik, and D. Korošak, "Functional connectivity in islets of Langerhans from mouse pancreas tissue slices," PLoS Comput. Biol. **9**, e1002923 (2013).
[8]R. Markovič, A. Stožer, M. Gosak, J. Dolenšek, M. Marhl, and M. S. Rupnik, "Progressive glucose stimulation of islet beta cells reveals a transition from segregated to integrated modular functional connectivity patterns," Sci. Rep. **5**, 7845 (2015).
[9]M. Rubinov and O. Sporns, "Complex network measures of brain connectivity: Uses and interpretations," Neuroimage **52**, 1059–1069 (2010).
[10]M. A. Ravier, M. Guldenagel, A. Charollais, A. Gjinovci, D. Caille, G. Sohl, C. B. Wollheim, K. Willecke, J. C. Henquin, and P. Meda, "Loss of connexin36 channels alters β-cell coupling, islet synchronization of glucose-induced Ca^{2+} and insulin oscillations, and basal insulin release," Diabetes **54**, 1798–1807 (2005).
[11]R. K. P. Benninger, M. Zhang, W. S. Head, L. S. Satin, and D. W. Piston, "Gap junction coupling and calcium waves in the pancreatic islet," Biophys. J. **95**, 5048–5061 (2008).
[12]R. K. P. Benninger and D. W. Piston, "Cellular communication and heterogeneity in pancreatic islet insulin secretion dynamics," Trends Endocrinol. Metab. **25**, 399–406 (2014).
[13]M. G. Pedersen, R. Bertram, and A. Sherman, "Intra- and inter-islet synchronization of metabolically driven insulin secretion," Biophys. J. **89**, 107–119 (2005).

[14]N. Pørksen, "The in vivo regulation of pulsatile insulin secretion," Diabetologia **45**, 3–20 (2002).
[15]M. Perc, "Spatial decoherence induced by small-world connectivity in excitable media," New J. Phys. **7**, 252 (2005).
[16]M. Perc, "Effects of small-world connectivity on noise-induced temporal and spatial order in neural media," Chaos, Solitons Fractals **31**, 280–291 (2007).
[17]X. Sun, M. Perc, Q. Lu, and J. Kurths, "Spatial coherence resonance on diffusive and small-world networks of Hodgkin-Huxley neurons," Chaos **18**, 023102 (2008).
[18]O. V. Aslanidi, O. Mornev, O. Skyggebjerg, P. Arkhammar, O. Thastrup, M. Sørensen, P. Christiansen, K. Conradsen, and A. Scott, "Excitation wave propagation as a possible mechanism for signal transmission in pancreatic islets of Langerhans," Biophys. J. **80**, 1195–1209 (2001).
[19]A. Stožer, J. Dolenšek, and M. S. Rupnik, "Glucose-stimulated calcium dynamics in islets of Langerhans in acute mouse pancreas tissue slices," PLoS One **8**, e54638 (2013).
[20]A. Sherman, "Contributions of modeling to understanding stimulus-secretion coupling in pancreatic beta-cells," Am. J. Physiol. **271**, E362–E372 (1996).
[21]A. Nittala, S. Ghosh, and X. Wang, "Investigating the role of islet cytoarchitecture in its oscillation using a new beta-cell cluster model," PLoS One **2**, e983 (2007).
[22]M. Pérez-Armendariz, C. Roy, D. C. Spray, and M. V. Bennett, "Biophysical properties of gap junctions between freshly dispersed pairs of mouse pancreatic beta cells," Biophys. J. **59**, 76–92 (1991).
[23]Q. Zhang, J. Galvanovskis, F. Abdulkader, C. J. Partridge, S. O. Göpel, L. Eliasson, and P. Rorsman, "Cell coupling in mouse pancreatic beta-cells measured in intact islets of Langerhans," Philos. Trans. A: Math., Phys. Eng. Sci. **366**, 3503–3523 (2008).
[24]M. G. Pedersen, "Homogenization of heterogeneously coupled bistable ODE's—Applied to excitation waves in pancreatic islets of Langerhans," J. Biol. Phys. **30**, 285–303 (2004).
[25]See supplementary material at http://dx.doi.org/10.1063/1.4949020 for five supplementary figures and a complete description of the model equations and parameters.
[26]V. Latora and M. Marchiori, "Efficient behavior of small-world networks," Phys. Rev. Lett. **87**, 198701 (2001).
[27]S. C. van der Marck, "Percolation thresholds and universal formulas," Phys. Rev. E **55**, 1514 (1997).
[28]P. Smolen, J. Rinzel, and A. Sherman, "Why pancreatic islets burst but single β cells do not. The heterogeneity hypothesis," Biophys. J. **64**, 1668–1680 (1993).
[29]A. K. Kryukov, V. S. Petrov, L. S. Averyanova, G. V. Osipov, W. Chen, O. Drugova, and C. K. Chan, "Synchronization phenomena in mixed media of passive, excitable, and oscillatory cells," Chaos **18**, 037129 (2008).